

**Original Research Article****DOI:10.26479/2019.0501.68**

## **DETERMINATION OF INDIGO CARMINE AT POLY (ADENINE) MODIFIED CARBON NANOTUBE PASTE ELECTRODE**

**Pushpanjali P A<sup>1</sup>, Manjunatha J G<sup>1\*</sup>, Raril C<sup>1</sup>, Ravishankar D K<sup>2</sup>**

1. Department of Chemistry, FMKMC College, Madikeri, Mangalore University  
Constituent College, Karnataka, India.
2. Department of Chemistry, Sri Mahadeshwara Government First Grade College,  
Kollegal, University of Mysore, Karnataka, India.

**ABSTRACT:** An electrocatalytic method was developed for the acute and selective determination of Indigo carmine (IC) using poly (Adenine) fabricated carbon nanotube paste electrode (PAMCNTPE). This modified electrode delineated the excellent current sensitivity towards the redox reaction of IC compared to bare carbon nanotube paste electrode (BCNTPE). Cyclic voltammetry (CV) study disclosed that this PAMCNTPE have quasi-reversible redox behavior in electrolyte solution. The electron transition kinetics on the electrode has been evaluated along with the variation of scan rate, concentration and pH. The surface morphology of the electrodes were characterized using field emission scanning electron microscopy (FESEM). The single and simultaneous determination of IC, Methyl Orange (MO) and Tartrazine (TZ) was executed using CV. The electrocatalytic behavior of IC at BCNTPE and PAMCNTPE in differential pulse voltammetry (DPV) was inspected. The calibration curve for IC gives a linear response in the range of  $8 \times 10^{-6}$  to  $1.3 \times 10^{-4}$  M in 0.2 M Phosphate buffer solution (PBS) at pH 8.0 with detection limit (LOD)  $2.7 \times 10^{-7}$  M and limit of quantification (LOQ)  $9.3 \times 10^{-7}$  M. The fabricated electrode exhibited high sensitivity, selectivity, stability and was successfully adapted for the determination of IC in the real sample.

**KEYWORDS:** Carbon Nanotube based sensor; Indigo Carmine; poly (Adenine); Electro polymerization; Cyclic Voltammetry.

**Corresponding Author: Dr. Manjunatha J G\* Ph.D.**

Department of Chemistry, FMKMC College, Madikeri, Mangalore University  
Constituent College, Karnataka, India. Email Address: manju1853@gmail.com

## 1. INTRODUCTION

Dyes are the coloured compounds which can be extracted from natural sources or can be synthesized in a laboratory. Synthetic dyes are used as colouring agents in many industries like pharmaceuticals, cosmetics, pulp and paper, printing, textile, paint, plastic and food industries [1]. In the worst side, their degradation products are highly toxic, dangerous or even mutagenic to living beings [2]. Therefore, great endeavor is necessary for developing potent analytical approaches for the determination of dyes [3]. IC is used as a redox indicator, which turns yellow on reduction. It is used as a dye in the manufacturing of capsules. IC is deliberated as a highly toxic indigoid class of dye and comprises one of the most influential group of contaminant found in wastewaters from textile industries. It was used in many industries, such as textile, plastics and papers industries, and it is used as indicator in analytical chemistry, as food colorant and as microscopic stain in biology [4]. TZ and MO are the azo dyes, these may be present in common food products which can cause diarrhea, allergies, migraines and even cancer if they are extravagantly consumed [5]. Detection and determination of these dyes in early ailment states are essential for public health safeguard [6]. In the present sequence, the insistence for biosensors of high sensitivity, selectivity and stability were expeditiously rising [7–8]. Nanoparticles seize numerous distinguishing physical and chemical aspects which make them convincing synthetic scaffold to embellish the detection systems in the sensors [9–10]. In recent times, nanocomposite modified electrodes are most oftenly used in biosensors, as this usage brings about variation in particle size, shape, surface morphology, chemical, and physical properties along with catalytic activity and chemical selectivity [11–14]. Numerous analytical techniques have been chosen for the determination of synthetic dyes, such as spectrophotometry, stripping voltammetry capillary electrophoresis, high-performance liquid chromatography with UV-VIS, UV-DAD or MS detectors for the individual and simultaneous determination of these dyes [15–23]. CV is the first technique enforced in an electrochemical inspection based on potential control and is more applicable in the study of redox reactions [24]. It is the most proficient electroanalytical tool for the analysis of drugs and biologically active compounds [25–27]. The present work gives the new voltammetric technique for the individual and simultaneous determination of IC, MO, and TZ. This technique includes low cost, a simple and sensitive procedure for the determination of IC using CV and DPV.

## 2. MATERIALS AND METHODS

### Reagents

Adenine, IC, MO, TZ were purchased from Molychem, Mumbai, India and multiwalled carbon nanotubes (external diameter 30-50 nm and length 10-30  $\mu\text{m}$ ) from Sisco Research Laboratory Pvt. Ltd. Maharashtra and were used as received. All other chemicals were of analytical grade quality and were used without further purification. The standard stock solutions of 0.2 M  $\text{Na}_2\text{HPO}_4$  and 0.2 M  $\text{NaHPO}_4$  were mixed in calculated proportion for the preparation of 0.2 M PBS. Freshly

prepared solutions of IC, MO, and TZ were used in all experiments and were prepared with distilled water.

### Apparatus

The electroanalyser of model EA-201 Chemilink system was used for all electrochemical measurements. All electrochemical measurements were carried out with a conventional three-electrode system. The PAMCNTPE or BCNTPE was used as a working electrode. A saturated calomel electrode (SCE) was used as the reference electrode and a platinum electrode used as the auxiliary electrode. All the assessments were carried out at room temperature (25°C).

### Preparation of BCNTPE

The preparation of bare carbon nanotube paste (BCNTP) was done by blending carbon nanotubes and silicone oil in the proportion 60:40 (w/w) using a mortar and pestle until a uniformly wetted paste was obtained. The cavity (3 mm internal diameter) of the working electrode was then packed with the prepared BCNTP. The surface of the electrode was refined using smooth paper. The electrical contact was made by connecting a copper wire to the paste at the end of the tube. For each assessment, the surface of the electrode was revived.

### Fabrication of PAMCNTPE

$0.25 \times 10^{-4}$  M Adenine was taken in the electrochemical cell containing PBS of 6.5 pH. The polymer film-modified electrode was fabricated by electrochemical polymerization of Adenine by CV in the potential range from 0 to 1600 mV at a sweep rate of 100 mV/s for 10 cycles. Fig.1 shows the cyclic voltammogram obtained for electropolymerization. After 10 cycles, the removal of physically adsorbed material was achieved by washing the electrode surface with distilled water.

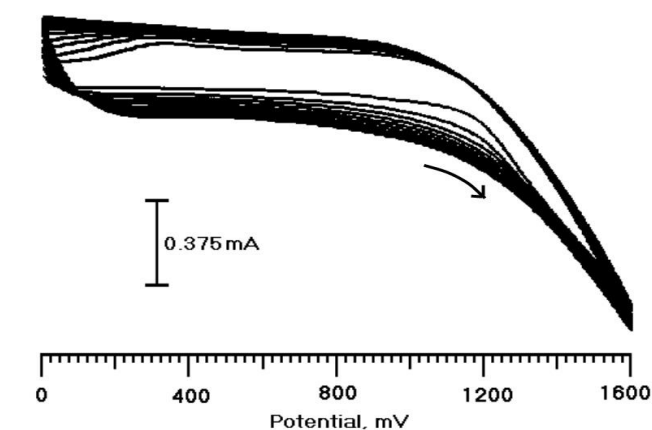


**Fig. 1: Cyclic voltammogram for the electrochemical polymerization of  $0.25 \times 10^{-4}$  M Adenine on a CNTPE in 0.2 M PBS (pH 6.5) at 10 cycles with sweep rate 100 mV/s.**

## 3. RESULTS AND DISCUSSION

### Surface morphology of BCNTPE and PAMCNTPE

The morphological characteristics were examined using FESEM images of BCNTPE and PAMCNTPE. Fig.2a and 2b depicted the morphological attributes of BCNTPE and PAMCNTPE

respectively. The surface of BCNTPE was observed to be coarse and contains uneven shaped nano-sized tubes of carbon nanotubes, whereas PAMCNTPE contains squishy like surface which confirms the formation of poly (adenine) film. This film is responsible for the enhancement of the electrocatalytic property.

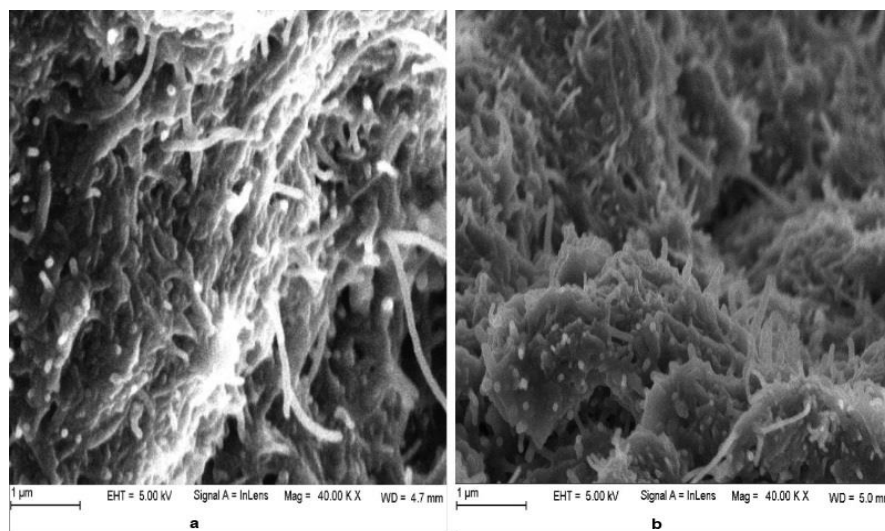


**Fig.2. FESEM images of (a) BCNTPE (b) PAMCNTPE.**

### Electrocatalytic response of IC

The electrochemical kinetics of the redox reaction of IC was investigated using the electrochemical measuring technique CV at PAMCNTPE in 0.2 M PBS at pH 8.0. The Fig.3 shows the response in the presence of IC (dashed line) and in the absence of IC (solid line). The redox peaks were observed for IC at PAMCNTPE in the potential range from 0 to 600 mV, but no characteristic peak was observed at PAMCNTPE in the absence of IC. When IC ( $1 \times 10^{-4}$  mol/L) was added to the 0.2 M PBS, a characteristic larger peaks corresponding to anodic and cathodic current at potentials 296 and 235 mV was observed. This electrochemical approach indicates that, the oxidation of the electroactive species produced by the reaction was proportional to the electrode response. The redox reaction of IC is shown in Fig.4 [28].

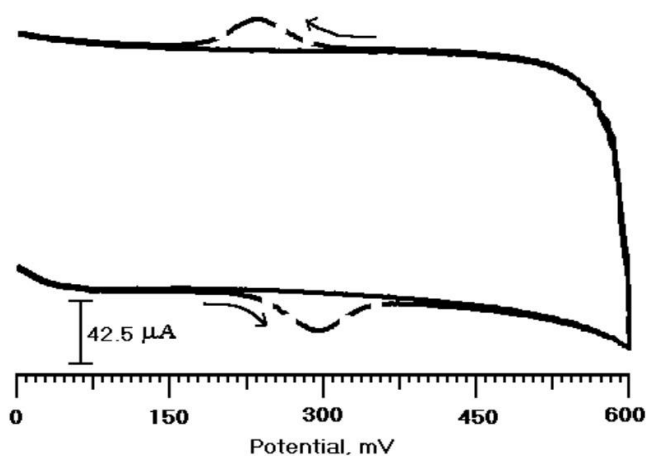


**Fig.3. A typical cyclic voltammograms of PAMCNTPE with  $1 \times 10^{-4}$  M IC in pH 8.0 PBS (dashed line) without  $1 \times 10^{-4}$  M IC at pH 8.0 PBS (solid line).**

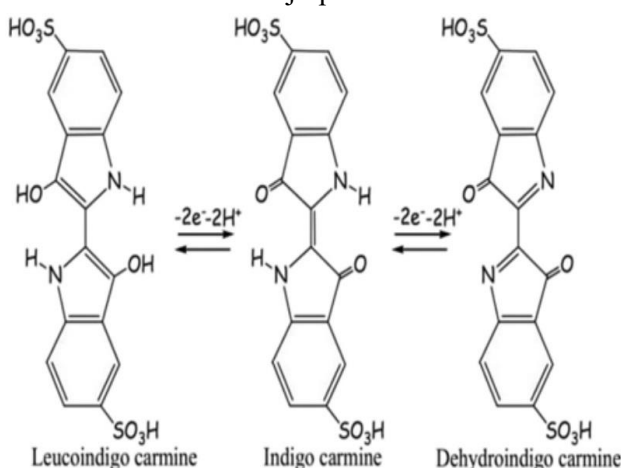


**Fig.4. The scheme of oxidation of IC**

### Electrocatalytic response of IC at PAMCNTPE

The cyclic voltammograms recorded with supporting electrolyte 0.2 M PBS at pH 8.0 with  $1 \times 10^{-4}$  M IC at BCNTPE and PAMCNTPE at the scan rate of  $75 \text{ mVs}^{-1}$  in the potential range from 0 to 600 mV (Fig.5). It was observed that there is no peak for IC at BCNTPE (solid line), while at the PAMCNTPE (dashed line), the well separated redox peak was observed with  $\Delta E_p = 61 \text{ mV}$ , which was higher than the value of  $59/n \text{ mV}$  expected for a reversible system and the ratio of redox peak current ( $I_{pa}/I_{pc}$ ) was 1.27, which were the characteristics of a quasi-reversible electrode process.

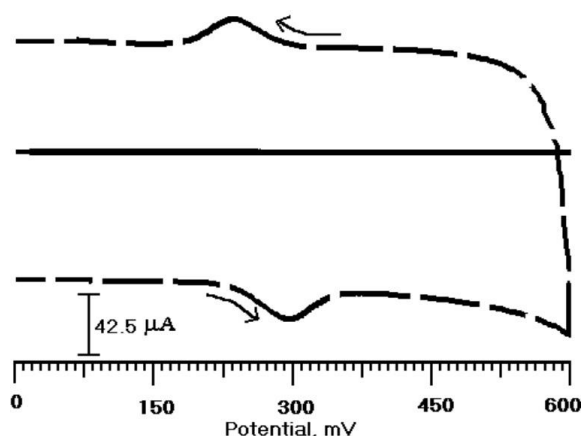


**Fig.5. Cyclic voltammograms of  $1 \times 10^{-4}$  M IC at the BCNTPE (solid line) and at the PAMCNTPE (dashed line) in 0.2 M PBS (pH 8.0).**

### Electrochemical Oxidation of IC by DPV at BCNTPE and PAMCNTPE

The DPV of IC at BCNTPE and PAMCNTPE obtained was showed in Fig.6. At PAMCNTPE (dashed line)  $1 \times 10^{-4}$  M IC exhibited sensitive response for electrochemical oxidation with peak potential and peak current 279 mV,  $104.4 \mu\text{A}$  respectively, but BCNTPE (solid line), does not showed any response for electrochemical oxidation of IC. These results showed that PAMCNTPE accelerates the characteristics of IC oxidation in 0.2 M PBS at pH 8.0.

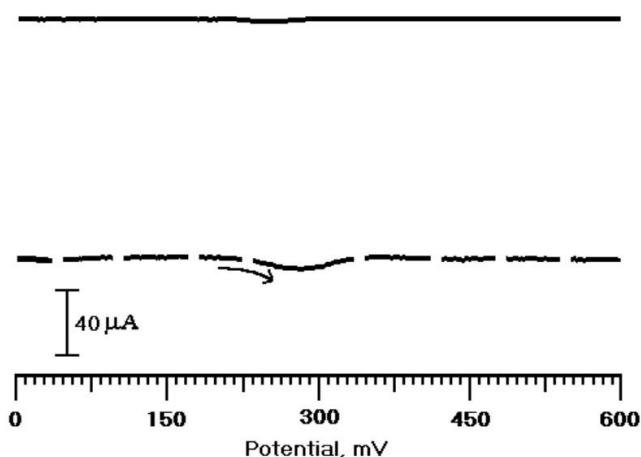


**Fig.6. DPVs of a solution containing  $1 \times 10^{-4}$  M IC in 0.2 M PBS (pH 8.0) at the BCNTPE (solid line), the PAMCNTPE (dashed line).**

### Impact of scan rate on the peak current of IC

By varying the scan rate from 75 to 250  $\text{mVs}^{-1}$ , the cyclic voltammograms of IC was recorded to study the influence of scan rate. Fig.7a indicates the great influence of scan rate on the peak current as well as peak potential of IC in 0.2 M PBS (pH 8.0) at PAMCNTPE. With the increase in the scan rate, the anodic peak current increases gradually and the anodic peak potential shifted to the more positive side. The graph obtained by plotting the anodic peak current ( $I_{pa}$ ) vs. scan rate showed a linear relationship (Fig.7b). The linear regression equation was  $I_{pa} (\mu\text{A}) = -61.177 + 1.979 v (\text{mVs}^{-1})$  with correlation co-efficient 0.999. The above data suggests that the electron transfer reaction in the solution was adsorption controlled.

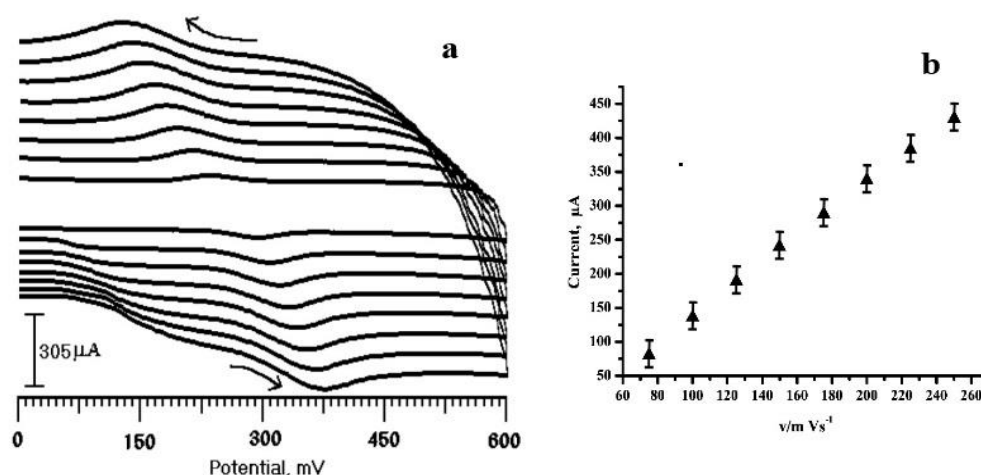


**Fig.7. (a) Cyclic voltammograms of  $1 \times 10^{-4}$  M IC at the PAMCNTPE in pH 8.0 PBS at various scan rates. From: 75-250  $\text{mV/s}$ . (b) The plot of the anodic peak current of IC as a function of scan rate.**

### Effect of pH on the oxidation of IC at PAMCNTPE

The influence of pH variation was investigated in the range from 6.0 to 9.0 in 0.2 M PBS using CV as shown in Fig.8a. The same electrode was used for the investigation of all the electrolytes. The anodic peak current was increased gradually from pH 6.0 and was get maximum at pH 8.0. Further, from 8.5 it goes on decreasing as shown in Fig.8b. This data was investigated at a scan rate 75 mV/s. Since, the highest peak current was obtained at pH 8.0, that particular pH buffer was chosen as the supporting electrolyte for the study of further parameters. Fig.8c showed that the relationship between anodic peak potential and pH. From the graph, it was observed that as the pH values increases, the anodic peak potential values shifted to the more negative side. The linear regression equation was  $E_{pa} \text{ (mV)} = 764.64 - 54.42 \text{ pH}$ , ( $r^2 = 0.995$ ).

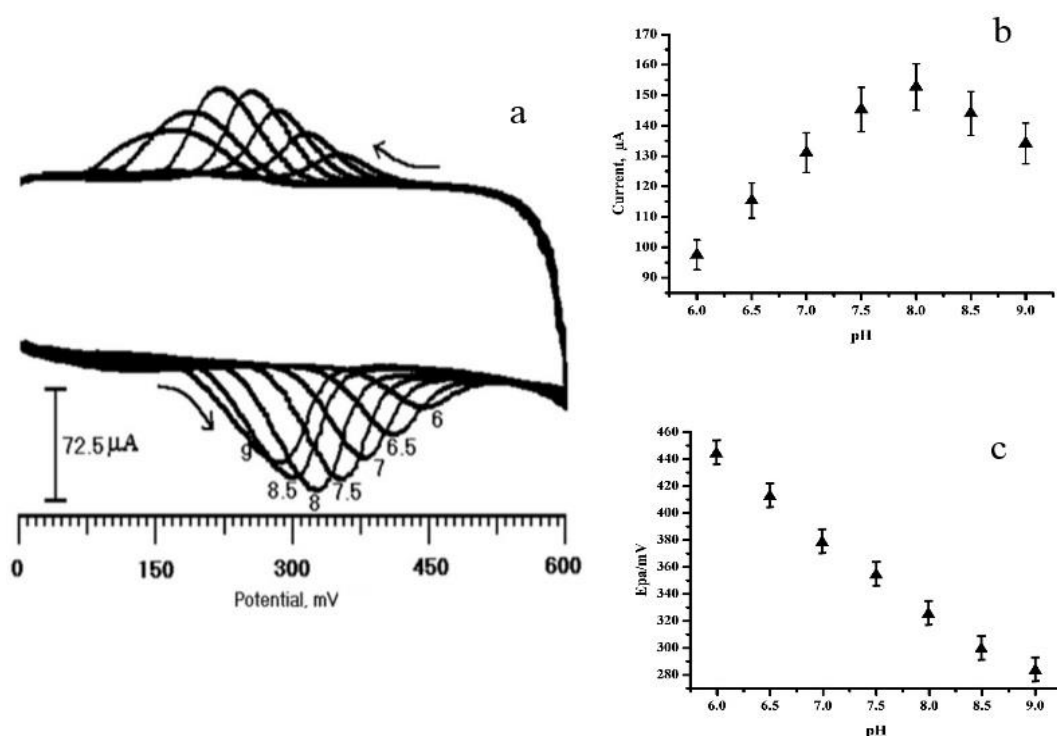


**Fig.8. (a) Cyclic voltammograms obtained at the PAMCNTPE in 0.2 M PBS in pH values, 6-9 containing  $1 \times 10^{-4}$  M IC. (b) The plot of anodic peak current vs. pH (6.0–9.0) of  $1 \times 10^{-4}$  M IC at the PAMCNTPE. (c) The plot of  $E_{pa}$  vs. pH for IC.**

### Electrochemical behavior of MO at BCNTPE and PAMCNTPE

The electrochemical behavior of  $1 \times 10^{-3}$  M MO at BCNTPE and PAMCNTPE was evaluated using CV technique. The cyclic voltammograms obtained are shown in Fig.9. BCNTPE does not show any response for MO in CV, but PAMCNTPE showed an oxidation peak for MO with anodic peak potential 627 mV corresponds to the anodic peak current 99.9 µA in 0.2 M PBS (pH 8.0). This result showed that the electrode response was equivalent to the oxidation of an electroactive species.

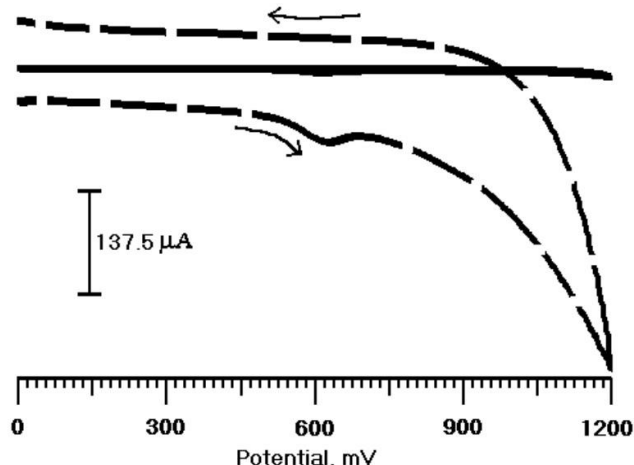


**Fig.9. Cyclic voltammograms of  $1 \times 10^{-3}$  M MO at the BCNTPE (solid line) and at the PAMCNTPE (dashed line) in 0.2 M PBS (pH 8.0).**

### Electrochemical behavior of TZ

CV occurred the oxidation peak for  $1 \times 10^{-3}$  M TZ in 0.2 M PBS (pH8.0) at PAMCNTPE with anodic peak potential, and peak current were 912 mV and  $185.1 \mu\text{A}$  respectively. At BCNTPE no peak was observed in CV. This result showed that the PAMCNTPE produce an excellent electrocatalytic activity towards TZ. The voltammogram obtained was showed in Fig.10. The presence of only anodic peak suggested that the reaction was irreversible.

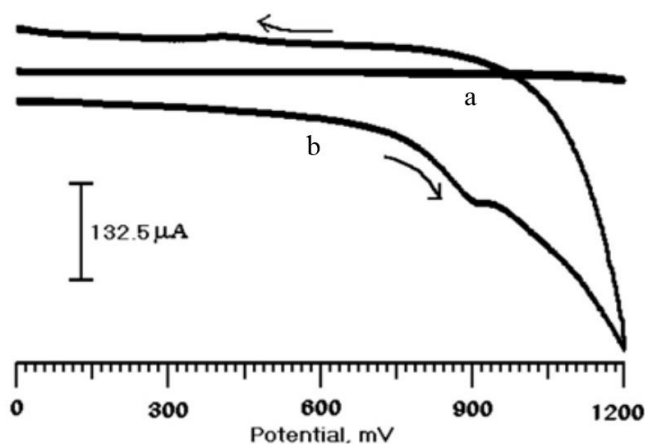


**Fig.10. Cyclic voltammograms of  $1 \times 10^{-3}$  M TZ at the BCNTPE (a) and at the PAMCNTPE (b) in 0.2 M PBS (pH 8.0).**

### Simultaneous detection of IC, MO, and TZ at PAMCNTPE

To examine the sensitivity and selectivity of the presently modified electrode for the quantitative determination of IC, MO and TZ, the electrochemical behavior was studied in the electrolyte containing the mixture of  $2 \times 10^{-4}$  M IC,  $2 \times 10^{-3}$  M MO and  $2 \times 10^{-3}$  M TZ using CV. Fig.11 indicates the response of IC, MO, and TZ at PAMCNTPE in 0.2 M PBS (pH 8.0) with anodic peak potential 296 mV, 627 mV and 913 mV respectively. This data indicated that the presently modified electrode has a good catalytic activity for the oxidation of IC, MO, and TZ and could clearly distinguish IC, MO and TZ.



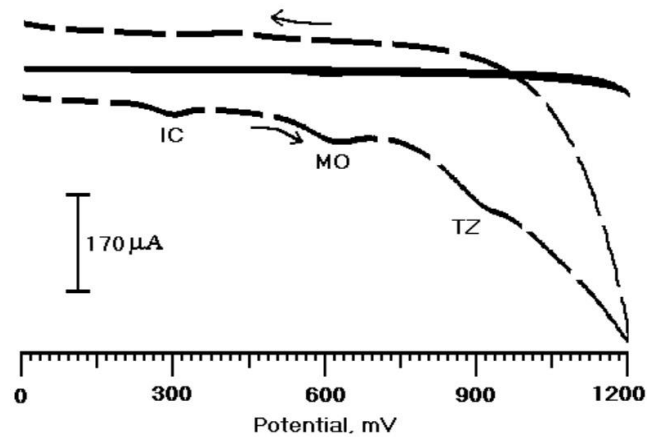


**Fig.11. Simultaneous determination of  $2 \times 10^{-4}$  M IC,  $2 \times 10^{-3}$  M MO and TZ at BCNTPE (solid line) and at PAMCNTPE (dashed line)**

#### Calibration curve and limit of detection for IC

The concentration of IC was determined at PAMCNTPE using CV. The investigation was performed for different concentration of IC ranges from  $8 \times 10^{-6}$  to  $1.3 \times 10^{-4}$  M in 0.2 M PBS at pH 8.0. The anodic peak current values corresponding to the oxidation of IC increased linearly with the increase in the concentration of IC. The plot of peak current vs. concentration of IC gives a straight line (Fig.12), with the linear regression equation  $I_{pa} \text{ (A)} = 6.065 \times 10^{-5} + 0.340 C \text{ (M)}$  ( $R=0.998$ ).

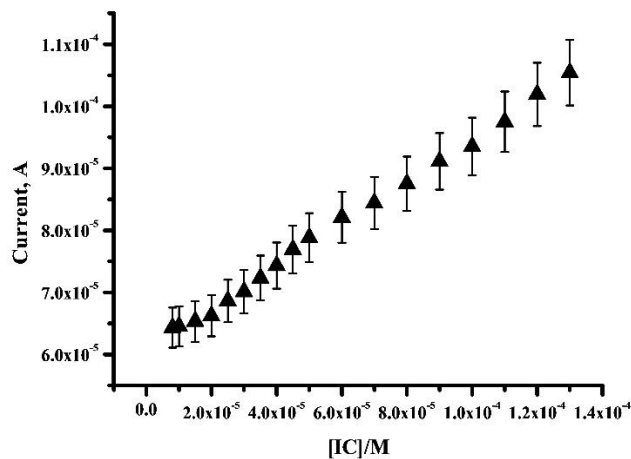


**Fig.12. Calibration plot for the determination of IC at the PAMCNTPE in pH 8.0 PBS with the scan rate 75 mV/s.**

The limit of detection (LOD) was calculated using the formula,  $LOD=3S_b/m$  and limit of quantification (LOQ) using  $LOQ=10S_b/m$ , where  $S_b$  is the standard deviation of the peak current of the blank solution (five replicants) and  $m$  is the slope of the calibration curve [29]. By substituting the values of  $S_b$  and  $m$  in the mentioned formula, the obtained values for LOD and LOQ were  $2.7 \times 10^{-7}$  M and  $9.3 \times 10^{-7}$  M respectively. The LOD values were compared with different reported electrodes [30–34], the present electrode showed some improvements, like low detection limits, long linear ranges and great current response (Table 1.).

© 2019 Life Science Informatics Publication All rights reserved

Peer review under responsibility of Life Science Informatics Publications

2019 Jan – Feb RJLBPCS 5(1) Page No.828

**Table 1. The comparison of PAMCNTPE with some other techniques for the determination of IC.**

Techniques	Linear range (mol/L)	Detection limits (mol/L)	Reference
Resonance Rayleigh scattering	$2 \times 10^{-6}$ – $32 \times 10^{-6}$	$2.4 \times 10^{-8}$	30
Spectrophotometry	$1.7 \times 10^{-6}$ – $39 \times 10^{-6}$	$2.5 \times 10^{-8}$	31
LC-APCI_MS	$2.1 \times 10^{-7}$ – $21 \times 10^{-7}$	$6.2 \times 10^{-8}$	32
SERRS	$1 \times 10^{-8}$ – $1 \times 10^{-5}$	$1.9 \times 10^{-5}$	33
Cyclic voltammetry	$2 \times 10^{-6}$ – $6 \times 10^{-5}$	$11 \times 10^{-8}$	34
Cyclic voltammetry	$8 \times 10^{-6}$ – $1.3 \times 10^{-4}$	$2.7 \times 10^{-7}$	This work

### Analytical application

Finally, to describe the usability of the biosensor in practical analysis, the proposed PAMCNTPE was applied to measure the IC content in commercial IC injection. The recovery test was also conducted. The analysis and recovery test demonstrate that our sensor offers an excellent in the range of 97–103%, accurate and precise method for the determination of IC in real samples.

### 4. CONCLUSION

The PAMCNTPE was subjected for the determination of IC and it exhibited an excellent electrocatalytic activity with a good current response. IC exhibits a redox reaction in the electrolyte, 0.2 M PBS (pH 8.0). This modified electrode was successfully incorporated for the individual and simultaneous determination of IC, MO, and TZ and have got well-separated peaks in cyclic voltammograms. IC was also investigated in the DPV technique. The easy preparation and high sensitivity of the presently modified electrode make the system highly applicable in pharmaceuticals, textile and in the food industry.

### ACKNOWLEDGEMENT

We gratefully acknowledge the financial support (KFIST) from the VGST, Bangalore under Research Project. No. KSTePS/VGST-KFIST (L1)2016-2017/GRD-559/2017-18/126/333, 21/11/2017.

### CONFLICT OF INTEREST

Author confirms no conflict of interest.

### REFERENCES

1. Robinson T, McMullan G, Marchant R, Nigam P. Remediation of dyes in textile effluent: A critical review on current treatment technologies with a proposed alternative. *Bioresour Technol.* 2001; 77(3):247–255.
2. Hastie J, Bejan D, Teutli-Leon M, Bunce NJ. Electrochemical methods for degradation of Orange II (sodium 4-(2-hydroxy-1-naphthylazo)benzenesulfonate). *Ind Eng Chem Res.* 2006;

45(14):4898–4904.

3. Ranade VV, Bhandari VM. Industrial wastewater treatment, recycling and reuse. Butterworth-Heinemann:Elsevier Science. 2014.
4. Ge L, Moor K, Zhang B, He Y, Kim JH. Electron transfer mediation by aqueous C<sub>60</sub> aggregates in H<sub>2</sub>O<sub>4</sub>/UV advanced oxidation of indigo carmine. *Nanoscale*. 2014; 6:13579–13585.
5. Rowe KS, Rowe KJ. Synthetic food coloring and behavior: a dose response effect in a double-blind, placebo-controlled, repeated-measures study. *J Pediatr*. 1994; 125:691–698.
6. Ilkhani H, Arvand M, Ganjali MR, Marrazza G, Mascini M. Nanostructured screen printed graphite electrode for the development of a novel electrochemical genosensor. *Electroanalysis*. 2013; 25(2):507–514.
7. Hamidi-Asl E, Daems D, De Wael K, Van Camp G, Nagels LJ. Concentration-related response potentiometric titrations to study the interaction of small molecules with large biomolecules. *Anal Chem*. 2014; 86(24):12243–12249.
8. Hejazi MS, Majidi MR, Gholizadeh S, Hamidi-Asl E, Turner APF, Golabi SM. Effect of electrophoresis on the efficiency of nano-TiO<sub>2</sub> modified silica sol-gel electrode. *J Nanosci Nanotechnol*. 2015; 15:3405–3410.
9. Perez-Lopez B, Merkoci A. Nanoparticles for the development of improved (bio)sensing systems. *Anal Bioanal Chem*. 2011; 399(4):1577–1590.
10. Manjunatha JG, Deraman M, Basri NH, Talib IA. Fabrication of poly (Solid Red A) modified carbon nano tube paste electrode and its application for simultaneous determination of epinephrin, uric acid and ascorbic acid. *Arab J Chem*. 2018; 11:149–158.
11. Chen KJ, Lee CF, Rick J, Wang SH, Liu CC, Hwang BJ. Fabrication and application of amperometric glucose biosensor based on a novel PtPd bimetallic nanoparticle decorated multi-walled carbon nanotube catalyst. *Biosens Bioelectron*. 2012; 33(1):75–81.
12. Lee KS, Son JM, Jeong DY, Lee TS, Kim WM. Resolution enhancement in surface plasmon resonance sensor based on waveguide coupled mode by combining a bimetallic approach. *Sensors*. 2010; 10(12):11390–11399.
13. Manjunatha JG, Deraman M, Basri NH, Nor NSM, Ataollahi N. Sodium dodecyl sulfate modified carbon nanotubes paste electrode as a novel sensor for the simultaneous determination of dopamine, ascorbic acid, and uric acid. *C R Chim*. 2014; 17(5):465–476.
14. Gholivand MB, Azadbakht A, Pashabadi A. An electrochemical sensor based on carbon nanotube bimetallic Au-Pt inorganic-organic nanofiber hybrid nanocomposite electrode applied for detection of guaifenesin. *Electroanalysis*. 2011; 23(12):2771–2779.
15. Ni YN, Gong XF. Simultaneous spectrophotometric determination of mixtures of food colorants. *Anal Chim Acta*. 1997; 354:163–171.
16. Berzas JJ, Rodriguez-Flores J, Villasenor Llerena MJ, Rodriguez Farinas N. Spectro-

- photometric resolution of ternary mixtures of tartrazine, patent blue V and indigo carmine in commercial products. *Anal Chim Acta*. 1999; 391:353–364.
17. Vidotti EC, Cancino JC, Oliveira CC, Rollemberg Mdo E. Simultaneous determination of food dyes by first derivative spectrophotometry with sorption onto polyurethane foam. *Anal Sci*. 2005; 21(2):149–153.
  18. Alghamdi AH. Determination of allura red in some food samples by adsorptive stripping voltammetry. *J AOAC Int*. 2005; 88(5):1387–1393.
  19. Suzuki S, Shirao M, Aizawa M, Nakazawa, Sasa K, Sasagawa H. Determination of synthetic food dyes by capillary electrophoresis. *J Chromatogr A*. 1994; 680(2):541–547.
  20. Masar M, Kaniansky D. Determination of synthetic dyes in food products by capillary zone electrophoresis in a hydrodynamically closed separation compartment. *J Capillary Electrophor*. 1996; 3:165–171.
  21. Dossi N, Toniolo R, Pizzariello A, Susmel S, Perennes F, Bontempelli G. A capillary electrophoresis microsystem for the rapid in-channel amperometric detection of synthetic dyes in foods. *J Electroanal Chem*. 2007; 601:1–7.
  22. Greenway GM, Kometa N, Macrae R. The determination of food colours by HPLC with on-line dialysis for sample preparation. *Food Chem*. 1992; 43:137–140.
  23. Ertas E, Ozer H, Cesarettin A. A rapid HPLC method for determination of Sudan dyes and Para Red in red chilli pepper. *Food Chem*. 2007; 105:756–760.
  24. Manjunatha JG, Deraman M. Graphene paste electrode modified with sodium dodecyl sulfate surfactant for the determination of Dopamine, Ascorbic acid and Uric acid. *Anal Bioanal Electrochem*. 2017; 9(1):198–213.
  25. Guo H, Lin H, Liu L, Song J. Polarographic determination of diazepam with its parallel catalytic wave in the presence of persulfate. *J Pharm Biomed Anal*. 2004; 34(5):1137–1144.
  26. Manjunatha JG. Electroanalysis of estriol hormone using electrochemical sensor. *Sens Biosensing Res*. 2017; 16:79–84.
  27. Hart JP. *Electroanalysis of biologically important compounds*. New York: Ellis Horwood Limited. 1990.
  28. Bond AM, Marken F, Hill E, Compton RG, Hu gel HJ. The electrochemical reduction of indigo dissolved in organic solvents and as a solid mechanically attached to a basal plane pyrolytic graphite electrode immersed in aqueous electrolyte solution. *Chem Soc Perkin Trans*. 1997; 2:1735–1742.
  29. Manjunatha JG. Surfactant modified carbon nanotube paste electrode for the sensitive determination of mitoxantrone anticancer drug. *J Electrochem Sci Eng*. 2017; 7(1):39–49.
  30. Li Q, Yang J, Tan X, Zhang Z, Hu X, Yang M. A simple and rapid resonance Rayleigh scattering method for detection of indigo carmine in soft drink. *Luminescence*. 2016; 31:1152–1157.

31. Berzas JJ, Rodriguez FJ, Villasenor Llerena MJ, Rodriguez Farinas N. Spectrophotometric resolution of ternary mixtures of tartrazine, patent blue V and indigo carmine in commercial products. *Anal Chim Acta*. 1999; 391:353–364.
32. Liao BC, Jong TT, Lee MR, Chen SS. LC-APCI-MS method for detection and analysis of tryptanthrin, indigo, and indirubin in daqingye and banlangen. *J Pharm Biomed*. 2007; 43:346–351.
33. Shadi IT, Chowdhry BZ, Snowden MJ, Withnall R. Semiquantitative analysis of indigo by surface enhanced resonance Raman spectroscopy (SERRS) using silver colloids. *Spectrochim Acta A*. 2003; 59:2213–2220.
34. Manjunatha JG. A novel poly (glycine) biosensor towards the detection of indigo carmine: A voltammetric study. *J Food Drug Anal*. 2018; 26(1):292–299.